JOC The Journal of Organic Chemistry

Article

pubs.acs.org/joc

Synthesis, Photophysical and Electrochemistry of Near-IR Absorbing Bacteriochlorins Related to Bacteriochlorophyll *a*

Andrei Kozyrev,*[,†] Manivannan Ethirajan,[‡] Ping Chen,[§] Kei Ohkubo,[⊥] Byron C. Robinson,[∥] Kathleen M. Barkigia,[¶] Shunichi Fukuzumi,*[,⊥,○] Karl M. Kadish,*[,§] and Ravindra K. Pandey*[,‡]

[†]Nanosyn, Inc., Santa Clara, California 95051, United States

[‡]Chemistry Division, PDT Center, Cell Stress Biology, Roswell Park Cancer Institute, Buffalo, New York 14263, United States

[§]Department of Chemistry, University of Houston, Houston, Texas 77204-5009, United States

[⊥]Department of Material and Life Science, Graduate School of Engineering, Osaka University, ALCA (JST), 2-1 Yamada-oka, Suita, Osaka 565-0871, Japan

[∥]Amgen, Thousand Oaks, California 91320-1799, United States

[¶]Brookhaven National Laboratory, Upton, New York 11973, United States

[○]Department of Bioinspired Science, Ewha Womans University, Seoul 120-750, Korea

Supporting Information

ABSTRACT: A series of new bacteriochlorins was synthesized using 13^2-oxo-bacteriopyropheophorbide *a* (derived from bacteriochlorophyll *a*) as a starting material, which on reacting with *o*-phenylenediamine and 1,10-diaminonaphthalene afforded highly conjugated annulated bacteriochlorins with fused quinoxaline, benzimidazole, and perimidine rings, respectively. The absorption spectra of these novel bacteriochlorins demonstrated remarkably red-shifted intense Q_y absorption bands observed in the range of 816−850 nm with high molar extinction coefficients (89,900−136,800). Treatment of 13^2-oxo-bacteriopyropheophorbide *a* methyl ester with diazomethane resulted in the formation of bacterioverdins containing a fused six-membered methoxy-substituted cyclohexenone (verdin) as an isomeric mixture. The pure isomers which exhibit long-wavelength absorptions in the near-IR region (865−890 nm) are highly stable at room temperature with high reactivity with O_2 at the triplet photoexcited state and favorable redox potential and could be potential candidates for use as photosensitizers in photodynamic therapy (PDT).

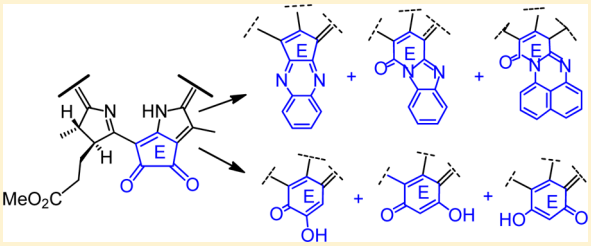

INTRODUCTION

Studies on porphyrins and related compounds as photosensitizers in the field of photodynamic therapy (PDT) suggest that long-wavelength absorbing chromophores may have advantages in destroying deeply seated tumors.[1,2] Porphyrin-based compounds with absorptions in the far red/near-IR region of the electromagnetic spectrum may have various applications as optical materials and sensors[3] or for PDT.[4] The availability of cheap LED diode lasers in the range of 800−900 nm will make PDT more economical and practical.[5] One approach used in the synthesis of long-wavelength absorbing compounds exploits the strategy of extending the π-conjugated macrosystem of the porphyrin chromophore.[6] This has been achieved by introducing fused aromatic rings directly attached to the porphyrin,[7] or by building extended cyclic pyrrolic macrocycles.[8,9] Another strategy that has been largely adopted utilizes partial reduction of the porphyrin system to produce chlorins or bacteriochlorins.[4] Introduction of electron-withdrawing substituents in such systems at an appropriate position(s) produces significant bathochromic shifts in their long-wavelength absorptions.[10] In some instances introduction of fused exocyclic ring(s), directly attached to the reduced porphyrinic skeleton, was found to be beneficial in shifting Q_y absorptions into the near-IR region.[11] Among tetrapyrrolic systems, bacteriochlorins are of particular interest, because they exhibit intense Q_y bands in the long-wavelength region.[12] Earlier, Dolphin and co-workers[13] and Pandey et al.[14] synthesized bacteriochlorins which possessed two fused rings on the opposite pyrrolic units and had long-wavelength absorptions in the range of 760−790 nm. Unfortunately, further studies on these chromophores have not been reported.

The synthesis of stable bacteriochlorins has been a challenging aspect of photosensitizer development in the field of PDT. A decade ago, Robinson et al.[15−17] reported the synthesis of a series of bacteriopurpurins, which had previously been erroneously reported as being so unstable that their characterization was not possible.[18] In this instance, it was found that the presence of two conjugated electron-withdrawing cyclopentenyl rings on the bacteriochlorins produced

Received: September 6, 2012
Published: October 22, 2012

Scheme 1

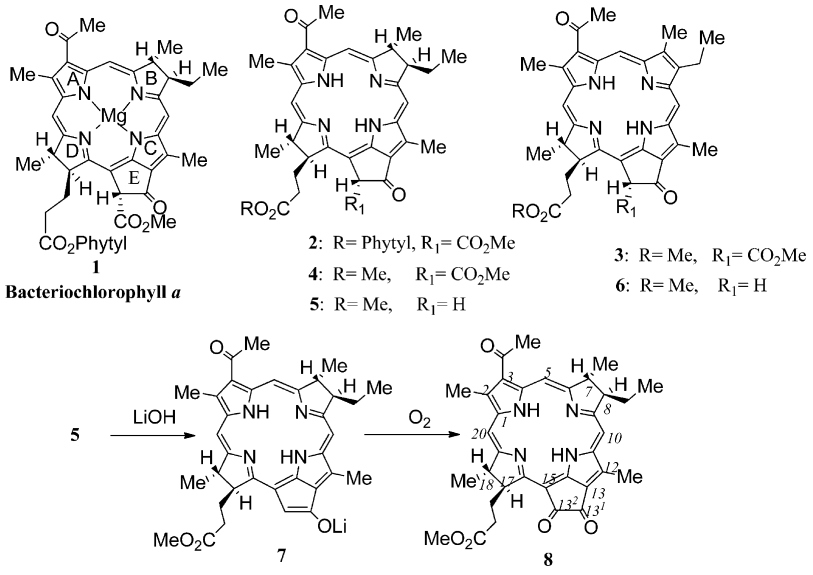

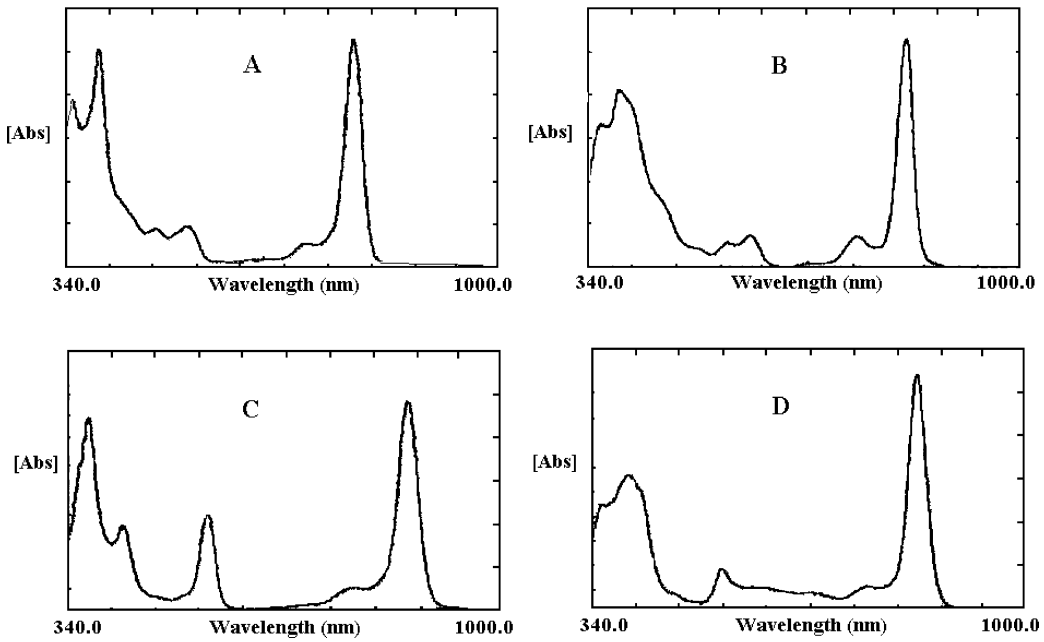

Figure 1. UV/near-IR absorption spectra (in CH_2Cl_2) of bacteriochlorins: (A) 13^2-oxo-bacteriopyropheophorbide *a* (**8**); (B) quinoxalino-bacteriochlorin (**10**); (C) benzimidazolo-bacteriochlorin (**11**); (D) perimidino-bacteriochlorin (**13**).

large bathochromic shifts of their Q_y-bands, which absorbed in the range of 846−863 nm.[17] A few years ago, Pandey and co-workers[19] extended the osmium tetroxide oxidation approach followed by the pinacol−pinacolone reaction in developing certain keto-bacteriochlorins derived from chlorins (pyropheophorbide a, chlorin e_6, and purpurinimide). A remarkable difference in photophysical properties and PDT efficacy was observed, depending on the position of the keto group at the position-7 or -8.

Natural bacteriochlorophylls, for example, bacteriochlorophyll *a* (**1**) and its derivatives, have been shown to possess significant potency as photosensitizers.[20] Many of these compounds appear to be unstable during in vivo experiments.[21] Bacteriochlorins with fused anhydride and imide rings have been reported to be more stable to photooxidation, while possessing adequate Q_y absorptions in the 800−820 nm range.[10,22] The utility of these compounds has been extensively investigated by Pandey and co-workers and some of the analogues have shown excellent PDT efficacy, both in vitro and in vivo in various tumor models.

The chemistry involving the enolization of pyropheophorbide was outlined by Pandey and co-workers[23] who showed the utility of the resulting product in highly conjugated systems. They followed this approach by first converting the bacteriochlorophyll *a* (**1**) to the corresponding α-diketone **8** which was then attached to a variety of fused aromatic moieties. This synthetic design followed the strategy of introducing moieties that extended conjugation on the pyrrolic unit C, while the opposite pyrrolic unit A contained an electron-withdrawing substituent (acetyl group). This arrangement of substituents along the pyrrolic A−C unit axis in bacteriochlorins was expected to provide large bathochromic effects on

dx.doi.org/10.1021/jo301895p | *J. Org. Chem.* 2012, 77, 10260−10271

Scheme 2

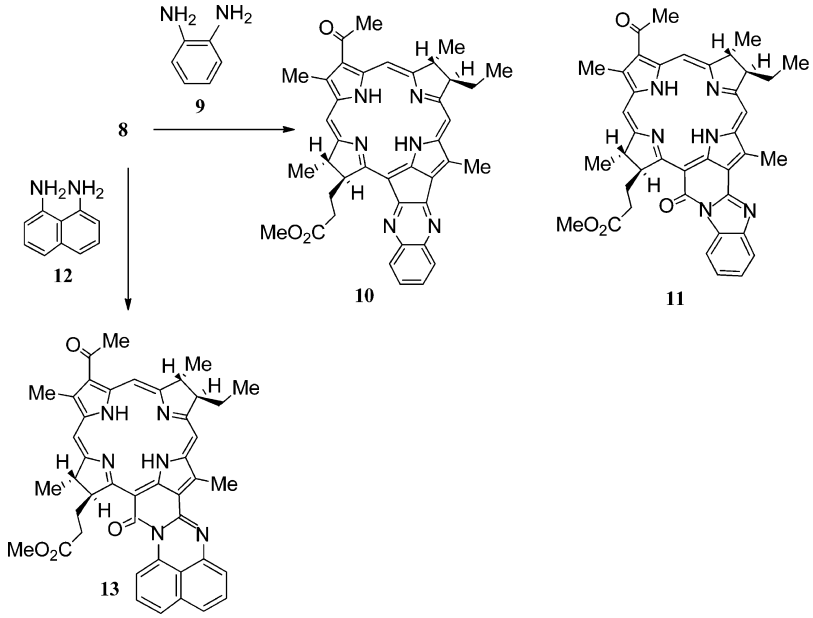

their Q_y absorption bands,[10] which could be shifted into the required near-IR region (above 800 nm). Here we report our results on the synthesis and spectroscopic, electrochemical, and photophysical characterization of a series of novel bacteriochlorins, bearing fused aromatic units.

RESULTS AND DISCUSSION

Annulated Aromatic Bacteriochlorins. Bacteriochlorophyll *a* (**1**) was isolated from *Rhodobacter sphaeroides* according to a standard procedure.[24] A brief treatment with 0.5% aq HCl afforded bacteriopheophytine *a* (**2**). Attempts to transesterify bacteriochlorin **2** using 2% sulfuric acid in methanol were unsuccessful, resulting in the formation of a significant amount (more than 50%) of 3-acetyl-3-devinyl-pheophorbide *a* (**3**). Other researchers have also reported difficulties working with bacteriochlorins in the presence of strong acids.[25,26] The phytyl ester group was cleaved efficiently using 80% aqueous TFA under an inert atmosphere,[25] and the resulting bacteriopheophorbide *a* was esterified using diazomethane to give methyl ester **4** in 89% yield.

A small amount of chlorin **3** (2%) was separated using chromatography on silica. Demethoxycabonylation of bacteriochlorin **4** in collidine afforded bacteriopyropheophorbide *a* (**5**) in 95% yield. A minor byproduct, isolated chromatographically as a faster moving band, was identified as 3-acetyl-3-devinyl-pyropheophorbide *a* (**6**) (3% yield). The synthesis of 13^2-oxo-bacteriopyropheophorbide *a* (**8**) followed the approach outlined for the autooxidation of related pyropheophorbide *a* and phylloerythrin compounds.[23] Hence, *in situ* autooxidation of the bacteriopyropheophorbide *a* (**5**) using aqueous LiOH in THF for 24 h followed by an acidic workup and re-esterification with diazomethane, afforded bacteriochlorin α-diketone (**8**) in 68% yield (see Scheme 1).[27] Surprisingly, no other oxidized byproducts (chlorins or porphyrins) or peripheral oxidation products were isolated from the reaction mixture as was observed in the LiOH-promoted allomerization of pyropheophorbide *a*.[23] As expected, bacteriochlorin (**8**) demonstrated a moderate bathochromic shift of the Q_y and Soret absorption bands, while the Q_x band was depressed and has a hypsochromic shift (Figure 1). The electron-withdrawing nature of the cyclopentyldiketone ring E produced a significant hyperchromic effect in the Q_y absorption band (768 nm, ε = 87,900) when compared to bacteriopyropheophorbide *a* (**5**) (754 nm, ε = 61,700). The presence of the 13^2-oxo-functionality was evident in the ^{1}H NMR spectrum of bacteriochlorin (**8**). Thus, when compared with similar resonances in **5**, the signal of the 17-H in **8** was shifted upfield to 5.00 ppm ($\Delta\delta$ = 0.97 ppm). The 13^2-methylene group resonance, which occurs at 5.33 ppm in **5**, was not observed in **8** as expected.

Condensation of bacteriochlorin **8** with 1,2-phenylenediamine **9** in pyridine in the presence of catalytic amounts of TFA[27−29] afforded two bacteriochlorins, which were isolated and purified by column and thin-layer chromatography. The minor product identified as quinoxalino-bacteriochlorin (**10**) (29%) based on HRMS and ^{1}H NMR spectroscopy data. A ^{1}H NMR spectrum of **10** displayed characteristic resonances from the aromatic protons of the quinoxaline fused ring at 7.49 and 7.96 ppm, while a mass ion (M + H) at m/z 653.3 was observed consistent with the structure.It was interesting to observe the effects induced by introduction of fused quinoxaline ring system in its UV−near-IR absorption spectrum (Figure 1). The extension of conjugation at ring E in bacteriochlorin **10** caused a significant bathochromic effect in the Q_y absorption band, shifted it to 816 nm. The high extinction coefficient (ε = 107,600) indicated a strong hyperchromic effect in the Q_y absorption band, due to the annulated polycyclic quinoxaline system in the chromophore **10**. The major product (54%) was identified as bacteriochlorin **11**, possessing a conjugated benzimidazole ring. The structure of this product was assigned on the basis of mass spectral and ^{1}H NMR data. Thus, the signal of the 17-H atom resonance at 5.43 ppm indicated the presence of the carbonyl function at the 13^3-position.[27] A similar deshielding effect on the 17-H resonance from the neighboring 13^3-keto group was reported in a bacteriopurpurin *a* imide series.[22] Signals from the aromatic protons of benzimidazole moiety resonated at δ 7.30, 7.86, and 8.06 ppm, which is similar in chemical shift to

dx.doi.org/10.1021/jo301895p | J. Org. Chem. 2012, 77, 10260−10271

Scheme 3

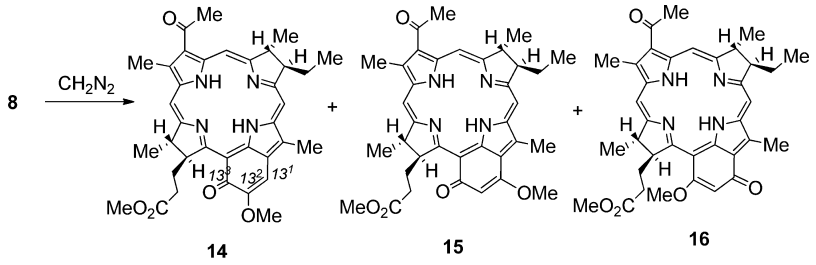

values reported in a pyropheophorbide *a* series.[28] By UV−near-IR spectroscopy, it is evident that the extended conjugation due to annulated benzimidazole in the bacteriochlorin chromophore **11** produced a large bathochromic shift ($\Delta\lambda$ = 96 nm) in the Q_y absorption (850 nm, ε = 89,800 M^{-1} cm^{-1}). The intense Q_x-band was also shifted to 553 nm (ε = 39,200 M^{-1} cm^{-1}). Presumably, bacteriochlorin **11** was formed as an autooxidized byproduct (allomer) during the condensation process.[28]

Using a similar synthetic methodology, condensation of bacteriochlorin **8** with 1,9-diaminonaphthalene **12** in pyridine/TFA gave perimidino-bacteriochlorin **13**, which was isolated as a sole product (79%) (Scheme 2). The annulated polycyclic perimidine moiety caused a remarkably large hyperchromic effect on the Q_y absorption band (829 nm, ε = 138,800 M^{-1} cm^{-1}), which has an extinction coefficient almost twice as large as its Soret band (398 nm, ε = 76,900 M^{-1} cm^{-1}) in the electron spectrum (Figure 1D). The exceptionally intense absorption maximum in bacteriochlorin **13** is a unique optical characteristic, which makes this chromophore very attractive for use as a recording material in information-storage media, or a dopant for nonlinear and luminescent optic materials. In contrast to bacteriochlorins **10** and **11** which are red in solutions, chromophore **13** displays broad absorption over 534−660 nm region, providing its solutions with a blue-green color.

Bacterioverdins. In the search for novel near-IR absorbing sensitizers, we were interested in exploring bacteriochlorins with various six-membered conjugated ring systems. It is known that the presence of a cyclohexenone (verdin) ring in chlorins and porphyrins produces significant bathochromic shifts in the Q_y absorption spectra of the molecules, ranging from 50 to 60 nm for porphyrins[30] and from 70 to 100 nm for chlorins.[31] The presence of the reactive *a*-diketone moiety in bacteriochlorin **8** provided an opportunity to introduce a verdin ring system to the bacteriochlorin chromophore, using a recognized diazomethane ring-enlargement approach.[32,33] Utilizing this synthetic methodology, we found that treatment of 13^2-oxo-bacteriopyropheophorbide *a* (**8**) with excess diazomethane at room temperature resulted in formation of three products (**14**−**16**) (Scheme 3), which were separated and purified chromatographically. Examination of the molecular weight for the compounds showed that each product had the same molecular ion at *m*/*z* 609.3, indicating that they were isomeric in nature and all possessed an annulated methoxycyclohexenone (verdin) ring system. As a new subclass of chromophores, we termed these compounds as *bacteriovervins*.

The structural assignment of bacterioverdins **14**−**16** was made using detailed 2D/ROESY ^{1}H NMR studies. The fastest moving band on silica was assigned to be the 13^2-methoxy-bacterioverdin (**14**), isolated in 29%. A 2D/ROESY ^{1}H NMR spectrum of **14** shows that the 13^1-H exhibits a strong through-space interaction with both signals associated with the 12-methyl and 13^2-methoxyl groups (Figure 2). By UV/near-IR spectroscopy, bacterioverdin **14** has a Q_y absorption band remarkably shifted into the near-IR region (891 nm, ε = 51,800 M^{-1} cm^{-1}). When compared to **5**, this represents a bathochromic shift of $\Delta\lambda$ = 137 nm, while the intensity of the Q_y absorption is slightly decreased. The Q_x-band was shifted to 550 nm and the Soret (B_1 and B_2) bands were observed at 368 and 423 nm (Figure 3). To our best of our knowledge, bacterioverdin **14** demonstrates the longest red-shifted Q_y absorption of any existing natural or synthetic bacteriochlorin derivative.[18]

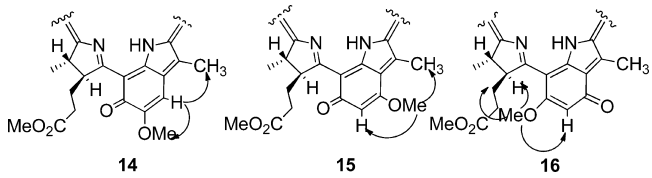

Figure 2. NOE interactions (selected) observed in 2D/ROESY ^{1}H NMR spectra of bacteriochlorins **14**−**16**.

The major product of the diazomethane ring enlargement reaction, isolated as the second fraction (42% yield), was assigned as the 13^1-methoxy-bacterioverdin (**15**). A ^{1}H NMR of this product showed a 17-H resonance at 5.18 ppm, clearly indicating the presence of a carbonyl function at the adjacent 13^3-position, as had been seen with bacteriochlorins **11** and **13**.

Additional evidence of its structure was provided by a 2D/ROESY ^{1}H NMR experiment, which showed distinctive interactions between resonances from the 13^1-methoxyl group and the 12-methyl substituent, as well as between the 13^1-methoxyl and the 13^2-H signals (Figure 2). As with isomer **14**, bacterioverdin **15** displays a Q_y absorption shifted to the near-IR region (874 nm, ε = 78,500 M^{-1} cm^{-1}), demonstrating a significant bathochromic effect ($\Delta\lambda$ = 120 nm).

The third and slowest eluting product of the diazomethane reaction was assigned as bacteriochlorin **16**, isolated in 16% yield. The 2D/ROESY ^{1}H NMR spectrum clearly shows that the resonance of the 13^1-methoxyl group exhibits strong through-space interactions with the neighboring 17-H and 13^2-H atoms (Figure 2). The multiplet attributed to the proton at the 17-position was observed at δ 4.78 ppm, indicating the absence of a neighboring carbonyl functionality at the 13^3-position in the verdin ring.[32] In contrast to bacterioverdins **14** and **15**, the ketone functionality in bacteriochlorin **16** is located at the 13^1-position; thus this product was termed as *bacterioisoverdin*. Bacterioisoverdin **16** has a Q_y absorption at 865 nm (ε = 48,600 M^{-1} cm^{-1}), while the Q_x band occurred at 596 nm. In contrast to bacterioverdins **14** and **15**, which are red

dx.doi.org/10.1021/jo301895p | J. Org. Chem. 2012, 77, 10260−10271

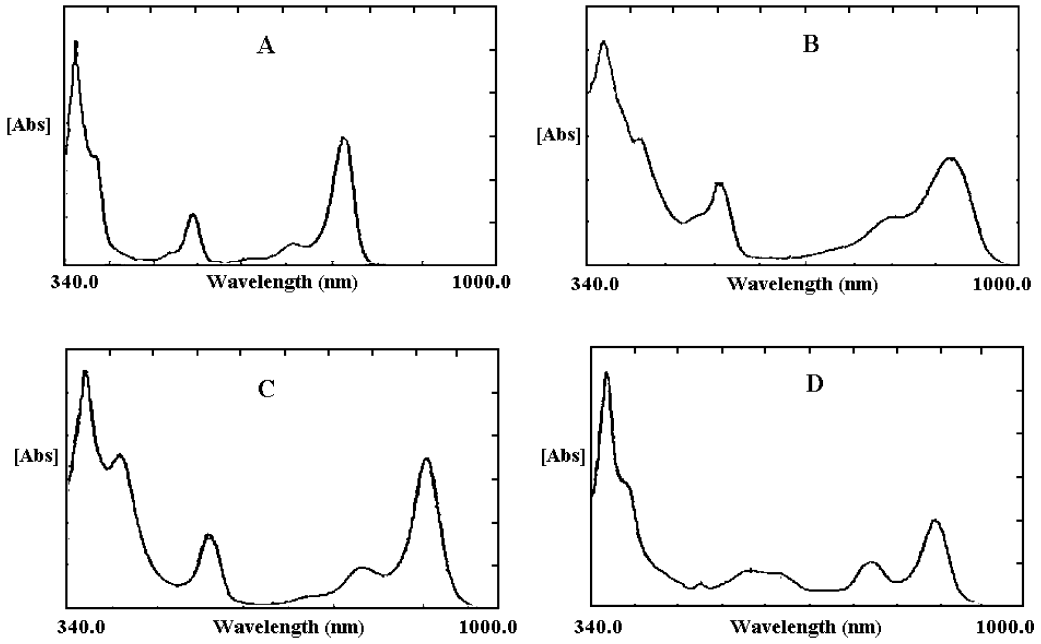

Figure 3. UV/near-IR absorption spectra (in CH_2Cl_2) of bacteriochlorins: (A) bacteriopyropheophorbide *a* **5**; (B) bacterioverdin **14**; (C) bacterioverdin **15**; (D) bacterioisoverdin **16**.

in solution, this compound has a characteristic deep-green color in solution (Figure 3).

An X-ray crystallographic determination of bacterioverdin **14** provided an unambiguous identification of its structure, in accord with independent 2D/ROESY ^{1}H NMR studies, and presents the first stereochemical parameters for this new class of bacteriochlorin. The compound crystallizes with three independent molecules in the unit cell, which display subtle differences in conformation and orientation of the side chains. Theoretical calculations based on the X-ray coordinates predict a range of 792−872 nm for the Q_y transition.[34] A view of the conformer that yields the best calculated agreement with the experimental value of 891 nm and presumably resembles most closely the conformation in solution is shown in Figure 4.

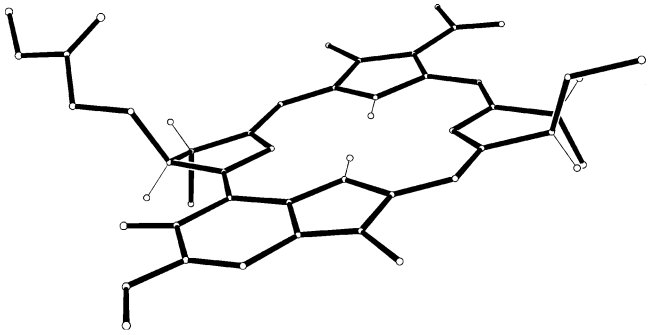

Figure 4. X-ray structure of bacterioverdin **14**. Peripheral substituents have been omitted for clarity.

Single crystals of **14** ($C_{36}H_{40}N_4O_5$) were grown from CH_2Cl_2/MeOH. Details and results of the X-ray experiment are included in CIF format in the Supporting Information. An analysis of the structures from the ring enlargement reaction sheds some light on the pathway of ring enlargement occurring within ring E (Scheme 4). Theoretically, it is possible that diazomethane reacts at both carbonyl functionalities to produce intermediates **17** and **18**. Both intermediates release nitrogen and produce ring enlargement by incorporating the methylene group between the 13^1- and 13^2-carbon atoms in the exocyclic ring E to give compound **20**, while ring enlargement between the 13- and 13^1, as well as 15-meso and 13^2-positions, should produce isomers **19** and **21**. The cyclohexanedione derivatives **19** and **20** should quickly enolize to produce verdins **21**−**23**, which on methylation via diazomethane should afford bacterioverdins **14**−**16**. Interestingly, the product **24** was not found among the isolated reaction products. Apparently, the absence of **24** indicates that the initial diazomethane attack takes place regioselectively at the 13^1-carbonyl function to form the only intermediate **17**, presumably due to the steric hindrance from the neighboring 17-propionic side chain. These data are consistent with earlier reports on the higher reactivity of the carbonyl at the 13^1-position.[29]

Electrochemistry. The electrochemical properties of seven bacterichlorins, **8**, **10**, **11**, and **13**−**16**, were examined in CH_2Cl_2 containing 0.1 M TBAP. Cyclic voltammograms are shown in Figure 5, and the redox potentials for each oxidation and reduction are listed in Table 1.

The investigated compounds undergo two reversible reductions at $E_{1/2}$ = −0.63 to −0.81 V and $E_{1.2}$ = −0.97 to −1.14 V, respectively, to form the radical anion and dianion. Two one-electron oxidations are also detected at $E_{1/2}$ = 0.61−0.81 V and E_p = 1.14−1.28 V to give the radical cation and dication. The first oxidation is reversible, while the second oxidation is quasi-reversible or irreversible due to the instability of the dication generated. However, two reversible oxidations can be observed at low temperatures, for these compounds and examples of cyclic voltammograms at −70 °C are shown in Figure 6 for compounds **10** and **14**. As shown in this figure, the second oxidation is located at $E_{1/2}$ = 1.10 V (**10**) or $E_{1/2}$ = 1.17 V (**14**), and side reactions are not observed after the second oxidation as is the case at room temperature. In addition, the first oxidation of **10** is split into two processes at the low temperature, probably due to aggregation of this compound, to a certain extent, under these experimental conditions.

dx.doi.org/10.1021/jo301895p | J. Org. Chem. 2012, 77, 10260−10271

Scheme 4. Possible Mechanism for the Formation of Bacterioverdins (21−23) from 13^2-Oxo-bacteriopyropheophorbide *a* (8)

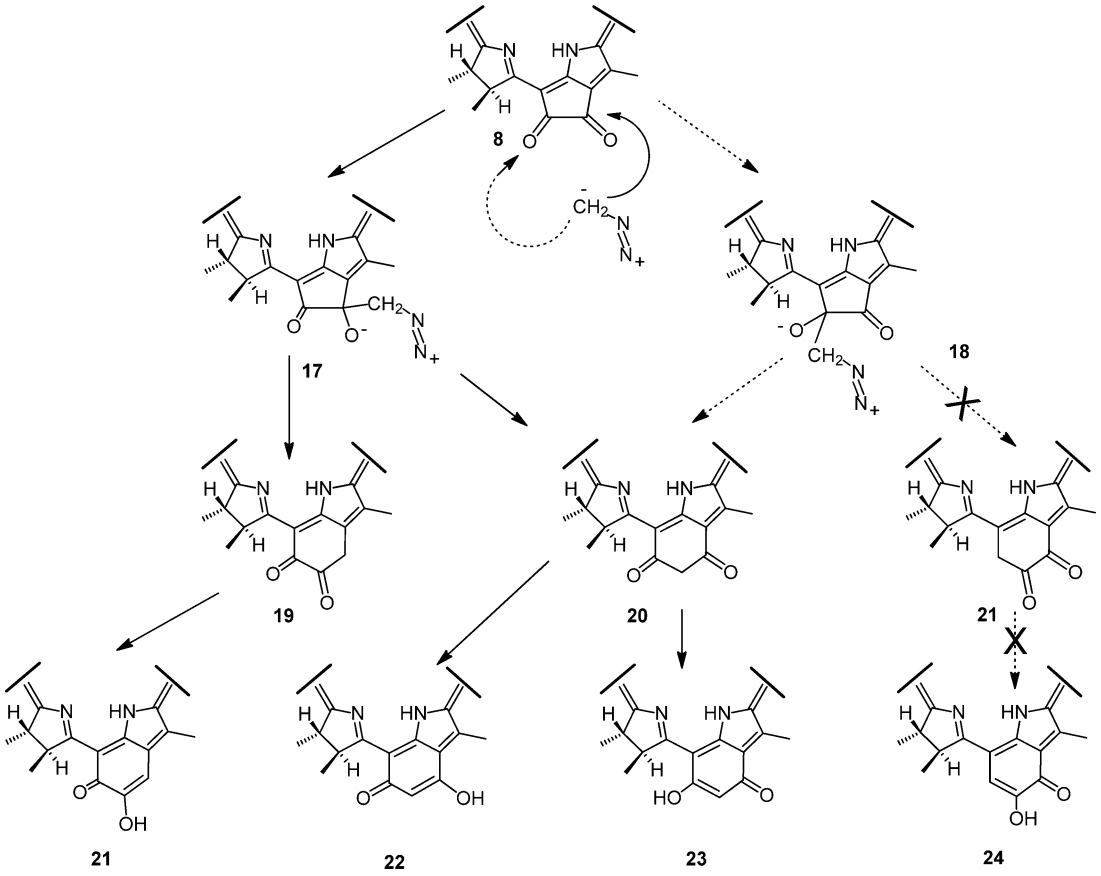

An almost constant potential difference between two reductions (Δred 1−2 = 0.33 ± 0.03 V) is observed for all compounds (see Table 1), while the potential difference between the first two oxidations is also similar for the examined compounds (Δox 2−1 = 0.51 ± 0.05 V). The electrochemical HOMO−LUMO gap of bacterichlorins in this series is 1.29−1.50 V. A similar HOMO−LUMO gap of 1.40 ± 0.05 V has been reported for other bacteriochlorin derivatives in our previous study.[35] These values are smaller than the gap of 1.52−1.60 V for metal-substituted bacteriochlorophyll *a*[36] and also much smaller than the gap of 1.90−2.10 V often seen for a number of nonplanar porphyrins.[37] It is worthy to point out that bacterioverdins **14**−**16** having a fused cyclohexenenone ring systems exhibit the smallest HOMO−LUMO gap (∼1.30 V). These three compounds also exhibit both the easiest reduction and the easiest oxidation as compared to other earlier studied compounds.

Spectroelectrochemistry. The electroreductions and electrooxidation of **8**, **10**, **11** and **13**−**16** were characterized by UV−vis thin-layer spectroelectrochemistry and the spectral data for the electrogenerated radical cations and radical anions of these bacteriochlorins are listed in Table 2. The spectral changes are reversible upon reversing the applied potentials, consistent with a high stability of the oxidized and reduced forms on the spectroelectrochemical time scale.

Examples of the UV−vis spectral changes obtained during the first two oxidations and first two reductions of compound **15** are illustrated in Figure 7. Upon the first reduction of **15** at −0.90 V (Figure 7a), the 369 nm Soret band and the strong 872 nm near-IR band decreased in intensity, while two weak bands grew in at 628 and 1039 nm. The NIR band at 1039 nm has been described as a marker band for the radical anion of bacteriochlorins and was predicted in MO calculations.[35,36] The first two controlled potential reductions for compound **15** are accompanied by reversible spectral changes in the thin-layer cell, and these spectra are shown in Figure 7b. As the electron transfer proceeds, the newly generated 628 and 1039 nm bands disappear, accompanied by the appearance of a weak and broad band at 564 nm, which is assigned to the bacteriochlorin dianion.

Three moderate intensity Soret bands are seen at 360, 398 and 429 nm, and there is a weak NIR band at 896 nm in the absorption spectrum of the radical anion for **15** (Figure 7c). The NIR band at 896 nm can be used as a marker band of the bacteriochlorin radical cation, and similar Soret bands were also reported in the radical cation spectrum of other bacteriochlorophyll derivatives.[35,36] This is due to the chlorine structure of the electrogenerated radical cation. A further oxidation of the radical cation **15** leads to a disappearance of the 360, 398, and 896 nm bands and the appearance of a stronger band at 448 nm when the controlled potential is switched to 1.30 V (Figure 7d).

Theoretical Study. Density functional theoretical (DFT) calculations were performed using the *Gaussian09* program (see Experimental Section), and the structures were optimized at the B3LYP/6-31+G(d,p) level of theory. The calculated HOMO−LUMO gaps are summarized in Table 3. There is a linear correlation between the HOMO−LUMO gaps obtained from electrochemical measurements and theoretical calculations as shown in Figure 8. The slope of the linear plot is 1.3, which indicates that there are no significant contributions of solvation to the redox behavior, due to the highly delocalized HOMO−LUMO on the macrocycle.

dx.doi.org/10.1021/jo301895p | *J. Org. Chem.* 2012, 77, 10260−10271

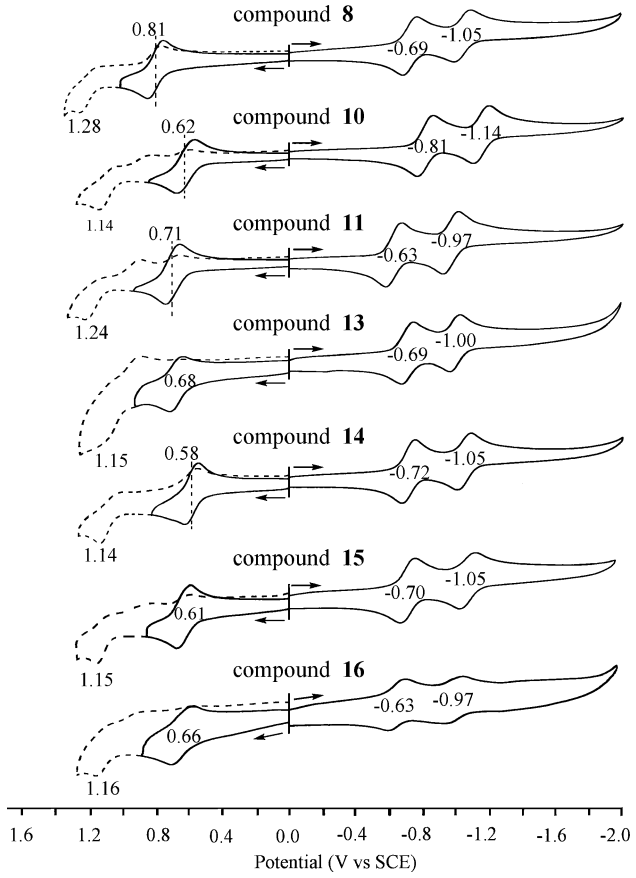

Figure 5. Cyclic voltammograms of compounds **8**, **10**, **11**, and **13**–**16** in CH_2Cl_2 containing 0.1 M TBAP at the scan rate of 0.1 V s^{-1}.

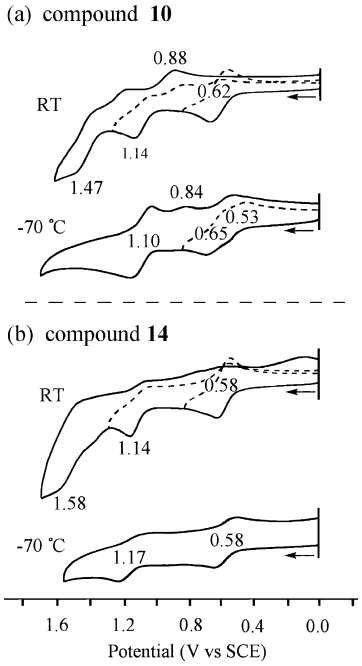

Figure 6. Cyclic voltammograms of compounds **10** and **14** in CH_2Cl_2 containing 0.1 M TBAP at room temperature and −70 °C.

Time-dependent DFT calculations using the optimized structure of DFT B3LYP/6-31+G(d,p) revealed the low-energy transition with the strong oscillator strength. The strong Q_y band in the near-IR region arises from the delocalized π-orbitals of the HOMO–LUMO. The near-IR transition obtained from TD-DFT ($h\nu$(DFT)) exhibits a linear correlation with the Q_y transition observed in CH_2Cl_2 ($h\nu$(obs)), as shown in Figure 9. The slope is close to unity (1.15).

Photophysical Properties. The dynamics of energy transfer from the triplet excited states of near-IR absorbing chlorines to dioxygen was examined by nanosecond laser flash photolysis measurements. Figure 10 shows a triplet–triplet (T-T) absorption band of **8** observed at 600 nm. Similar T-T absorption bands were observed for **9**-**12**. In the case of **13**, however, no T-T absorption band was observed probably due to the electron-transfer quenching of the singlet excited state by the naphthylamine donor moiety of **13**. The T-T absorption decay of **8** obeys first-order kinetics (Figure 10a), and this indicates that there is no contribution from the T-T annihilation under the present experimental conditions. The triplet lifetime was determined as 360 μs. The decay of the T-T absorption of **8** in air-saturated PhCN (Figure 10b) was enhanced significantly as compared with what is observed in deaerated PhCN (Figure 10a) because of energy transfer from the triplet excited state of **8** (^{3}**8***) to O_2. The rate constant of energy transfer from ^{3}**8*** to O_2 was determined to be 1.5×10^9 M^{-1} s^{-1}, which is smaller than the reported diffusion rate constant in PhCN.[37,38] The rate constants of the triplet decay and energy transfer to O_2 for other near-IR absorbing bacteriochlorins were determined similarly, and the results are listed in Table 4.

■ CONCLUSIONS

The synthesis of a series of novel bacteriochlorins related to bacteriochlorophyll *a*, possessing annulated heterocyclic systems was achieved. Through the careful synthetic design of introducing conjugated fused ring systems at the pyrrolic unit

Table 1. Half-Wave and Peak Potentials (V vs SCE) of Investigated Compounds (~10^{-3} M) in CH_2Cl_2 Containing 0.1 M TBAP under RT

	oxidation			reduction			
cmpd	Δox 2−1	2nd ox[a]	1st ox[b]	1st red[b]	2nd red[b]	Δred 1−2	HOMO–LUMO gap
8	0.47	1.28	0.81 (0.07)	−0.69 (0.08)	−1.05 (0.07)	0.36	1.50
10	0.52	1.14	0.62 (0.08)	−0.81 (0.08)	−1.14 (0.08)	0.33	1.43
11	0.53	1.24	0.71 (0.06)	−0.63 (0.09)	−0.97 (0.10)	0.34	1.34
13	0.47	1.15	0.68 (0.08)	−0.69 (0.06)	−1.00 (0.07)	0.31	1.37
14	0.56	1.14	0.58 (0.06)	−0.72 (0.08)	−1.05 (0.06)	0.33	1.30
15	0.54	1.15	0.61 (0.06)	−0.70 (0.07)	−1.05 (0.07)	0.35	1.31
16	0.50	1.16	0.66 (0.08)	−0.63 (0.06)	−0.97 (0.07)	0.34	1.29

[a] E_{pa} at a scan sate of 0.1 V s^{-1}. [b] $E_{1/2}$ ($\Delta E_p = E_{pa} - E_{pc}$ at a scan rate of 0.1 V s^{-1}).

dx.doi.org/10.1021/jo301895p | J. Org. Chem. 2012, 77, 10260–10271

Table 2. Thin-Layer Near-IR Spectral Data of Radical Anions and Cations of Investigated Compounds ($\sim 10^{-3}$ M) in CH_2Cl_2 Containing 0.1 M TBAP

	radical anion					radical cation				
cmpd	λ, nm ($\varepsilon \times 10^{-4}$ M^{-1} cm^{-1})[a]					λ, nm ($\varepsilon \times 10^{-4}$ M^{-1} cm^{-1})[a]				
8	364[s] (5.5)	378 (5.6)	584 (1.7)	768 (1.7)	906 (1.5)	348 (5.4)	396 (8.7)	518 (0.9)	770 (2.7)	836 (1.2)
10	363 (5.2)	403 (6.5)	601 (2.1)	816 (3.9)	908 (1.1)	365 (7.6)	406 (7.4)	582 (1.3)	730 (1.5)	817 (2.7)
11	376 (4.4)	557 (2.1)	615 (2.4)	852 (2.4)	1017 (1.5)	364 (5.7)	397 (5.7)	434 (6.2)	584 (1.2)	895 (1.8)
13	363 (4.2)	539 (2.8)	651 (3.1)	830 (2.3)	1018 (1.4)	353 (5.3)	413 (8.8)	589 (1.6)	833 (3.4)	885 (1.7)
14	365 (1.6)	381[s] (1.6)	544 (2.5)	644 (2.5)	889 (1.5)	353 (8.3)	398 (10.0)	434 (9.0)	800 (1.4)	885 (1.8)
15	374 (5.1)	398 (5.0)	572 (1.6)	628 (2.3)	1039 (1.1)	360 (8.0)	398 (8.8)	429 (9.3)	769 (0.7)	896 (1.3)
16	369 (6.2)	400 (5.2)	509 (1.4)	761 (1.8)	867 (1.4)	370 (7.3)	392 (6.3)	641 (1.6)	766 (1.4)	866 (1.9)

[a]Molar absorptivity (ε) of radicals is calculated by comparing the relative intensities of initial (neutral species) and final (radical) spectra, while the ε of the neutral species was obtained by a regular near-IR measurement in a 1 cm cell; s = shoulder.

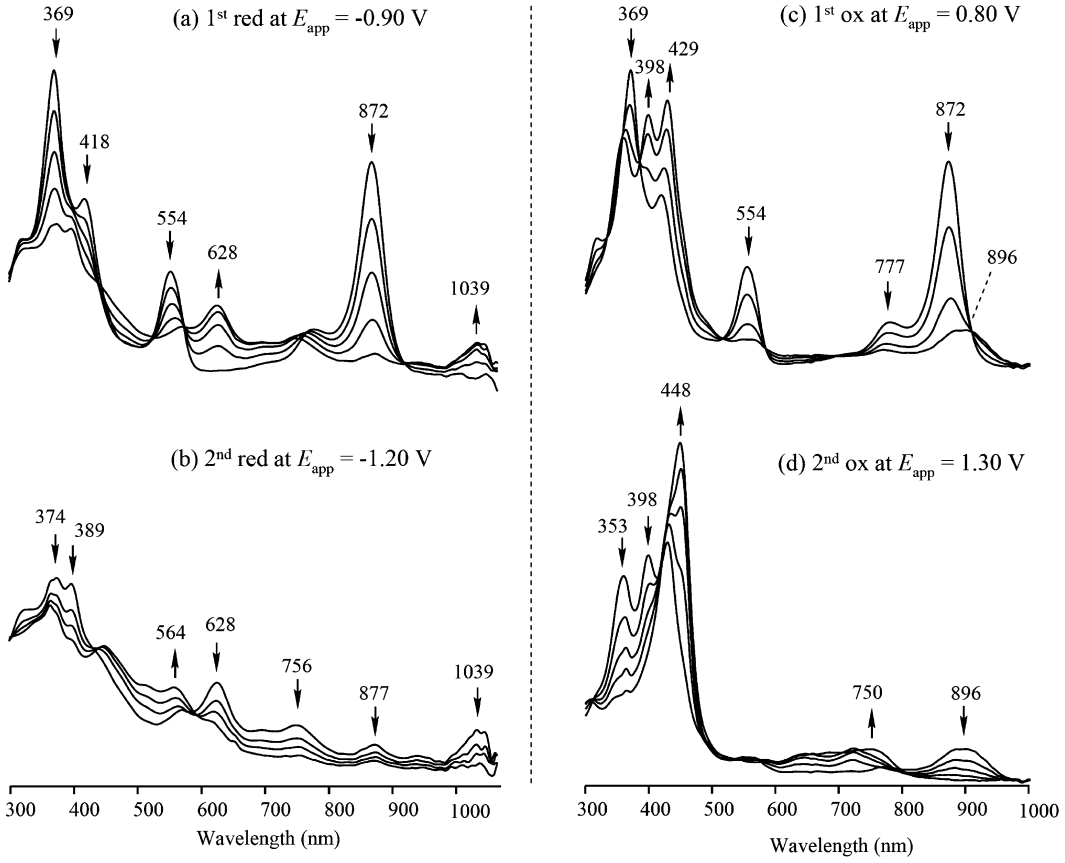

Figure 7. Near-IR spectral changes for (a) the first and (b) the second reductions, and (c) the first and (d) the second oxidations of compound **15** in a thin-layer cell at indicated potentials in CH_2Cl_2 containing 0.1 M TBAP.

Table 3. HOMO and LUMO Energies Determined from the DFT B3LYP/6-31+G(d,p) Level of Theory

cmpd	HUMO, eV	LUMO, eV	HOMO–LUMO gap
8	−5.35	−3.35	2.00
10	−5.02	−3.11	1.91
11	−5.19	−3.39	1.80
13	−5.13	−3.33	1.80
14	−5.00	−3.23	1.77
15	−4.96	−3.22	1.74
16	−5.08	−3.26	1.82

C, we were successful in preparing near-IR absorbing dyes. Spectroscopic data demonstrated that the outlined modifications resulted in large bathochomic shifts in the Q_y-absorption bands, accompanied by a significant hyperchromic effect in several derivatives. Presumably the nature of bathochromic shift could be explained as a result of a decrease in the energy gap between the HOMO and LUMO transitions.[38,39]

The observed bathochromic effects in the absorption spectra of these derivatives were largest in bacterioverdins **14**–**16**, which possess fused cyclohexenenone ring systems. These bacteriochlorins have Q_y absorptions in the near-IR region (870–890 nm), potentially making them attractive candidates as photosensitizers in the field PDT, especially for the treatment of target cells deeply located within tissues. Energy limitations in singlet oxygen generation likely make chromophores with long-wavelength absorptions above 900 nm nonpractical for PDT.[40] Possibly, bacterioverdins **14**–**16** possess the longest near-IR shifted absorptions, which could

dx.doi.org/10.1021/jo301895p | J. Org. Chem. 2012, 77, 10260–10271

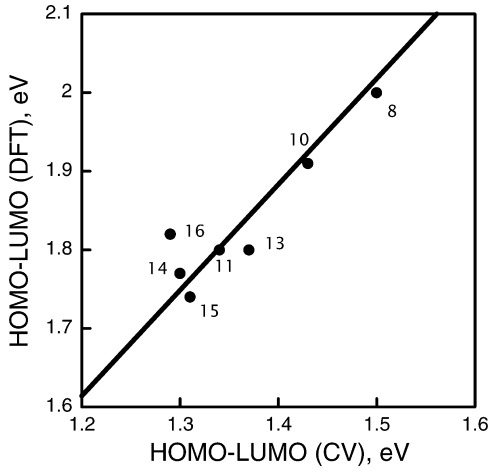

Figure 8. Plot of HOMO−LUMO gaps determined from CV and DFT calculations (B3LYP/6-31+G(d,p)).

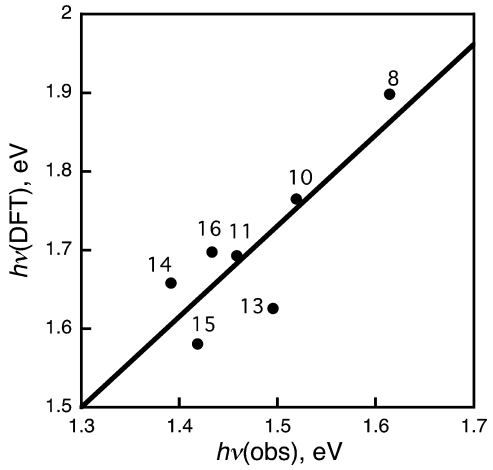

Figure 9. Plot of the transition energies determined from TD-DFT calculations (TDB3LYP/6-31+G(d,p)//B3LYP/6-31+G(d,p)) and electronic absorption spectra.

be used to achieve a photodynamic effect. Photochemical studies and biological testing of these novel bacteriochlorins are currently under investigation and will be reported elsewhere. The unique optical properties of the series of annulated bacteriochlorins make them attractive for other applications, including information-storage media and optical materials.[41] In addition, bacteriochlorin **8**, which possesses a reactive *a*-diketone functionality, could be useful also as a synthetic building block for the preparation of linear porphyrinic arrays and other photosynthetic models.[38]

EXPERIMENTAL SECTION

Preparative thin-layer chromatography was performed on 1 mm silica gel plates. Column chromatography was carried out using silica gel 60 (70−230 mesh). Purity of the isolated products after preparative chromatography was monitored using HPLC (RP-18 column) and UV−vis spectroscopy on spectrophotometer. ^{1}H NMR spectra were recorded using deuterochloroform as a solvent. Chemical shifts are reported in ppm downfield from tetramethylsilane as an internal standard. The peak assignments of compounds **14**−**16** were confirmed by two-dimensional (2D) (COSY, NOESY) methods. Fast atom bombardment (FAB) low- and high-resolution mass spectra were obtained on a double focusing, magnetic sector mass spectrometer. Nanosecond time-resolved transient absorption measurements were

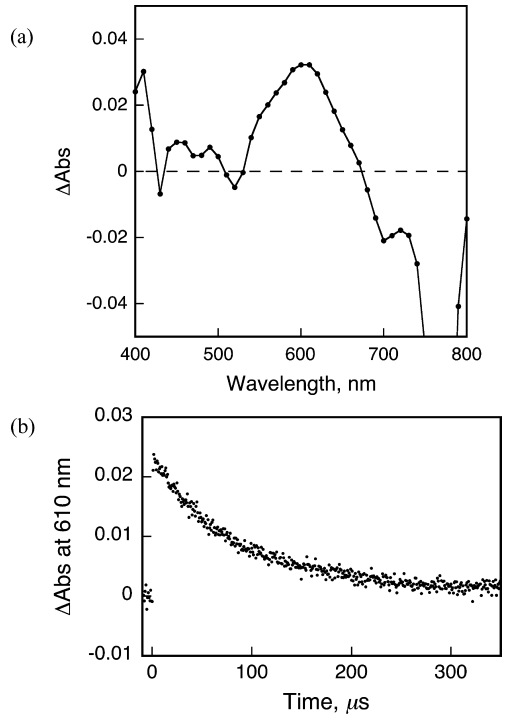

Figure 10. (a) T-T absorption spectrum of **8** (3.0×10^{-5} M) obtained by the laser flash photolysis in deaerated PhCN at 5.6 μs after laser excitation (562 nm) at 298 K. (b) Decay curves of transient absorbance at 610 nm of **8** (a) in the absence of O_2 and (b) in air-saturated PhCN ([O_2]) 1.7×10^{-3} M) at 298 K.

Table 4. Decay Rate Constants of the Triplet−Triplet Absorption under Argon and Air Atmosphere and Rate Constants of Energy Transfer from the Excited States to O_2 in PhCN at 298 K

cmpd	k_{obs}(argon), s^{-1}	k_{obs}(air), s^{-1}	k_{EN}, M^{-1} s^{-1}[a]
8	1.4×10^4	2.5×10^6	1.5×10^9
10	2.3×10^4	2.5×10^6	1.5×10^9
11	1.6×10^4	1.9×10^6	1.1×10^9
14	4.8×10^4	1.5×10^6	8.8×10^8
15	4.8×10^4	1.4×10^6	8.2×10^8
16	1.5×10^4	1.1×10^6	6.5×10^8

[a] $k_{EN} = (k_{obs}(\text{argon}) - k_{obs}(\text{air})]/[O_2]$. [$O_2$] under air is 1.7×10^{-3} M.[35]

carried out using the laser system. Measurements of the nanosecond transient absorption spectrum were performed according to the following procedure. A deaerated solution containing a compound was excited by a laser. The photodynamics were monitored by continuous exposure to a xenon lamp (150 W) as a probe light and a photomultiplier as a detector. The solution was oxygenated by nitrogen purging for 15 min prior to measurements. All new compounds decomposed >150 °C.

Theoretical Calculations. Density functional theory (DFT) calculations were performed with *Gaussian09* (Revision A.02)[42] The calculations were performed on a 32-processor QuantumCube at the B3LYP/lanl2dz level of theory.[43] Graphical outputs of the computational results were generated with the *GaussView* software program (ver. 3.09) developed by Semichem, Inc.[44] Electronic excitation energies and intensities were computed by the time-dependent (TD)-DFT calculation at the B3LYP/lanl2dz level.[42,45] The size of the integration grid used for all calculations was 10. In each case, 40 excited states were calculated by including all one-electron excitations

dx.doi.org/10.1021/jo301895p | J. Org. Chem. 2012, 77, 10260−10271

within an energy window of ±3 hartree with respect to the HOMO/LUMO energies.

Bacteriopheophorbide *a* Methyl Ester (4). *Rb. sphaeroides* biomass (200 mL) was suspended in 1-propanol (1.5 L) and stirred at room temperature, in the dark, with constant nitrogen bubbling for 12 h. The blue-green extract was filtered, and aq 0.5 N HCl (50 mL) was added to the filtrate. The reaction mixture was diluted with aq 5% NaCl (2 L) and extracted with dicloromethane (3 × 300 mL). The combined extracts were washed with water (3 × 500 mL), dried, and evaporated by rotary evaporation. The residue was precipitated from hexanes to give **bacteriopheophytine *a* (2)** (590 mg) with purity sufficient to proceed to the next step; UV−vis λ_{max} (Et_2O) nm 356, 383, 527, 749; [lit.[46] λ_{max} (Et_2O) nm ($\varepsilon \times 10^4$) 356 (11.3), 383 (6.27), 525 (2.83), 750 (6.75)]. Compound **2** was dissolved in aq 80% TFA (100 mL) and stirred in the dark at 0 °C for 2 h. The solution was then diluted with ice/water (500 mL) and extracted with dicloromethane (3 × 200 mL). The combined organic extracts were washed with water, treated with diazomethane, and evaporated to dryness. The crude residue was chromatographed on silica (eluent: dichloromethane−acetone, gradient 3−5% acetone) to give two bands. The minor, faster running band was **3-acetyl-3-desvinylpheophorbide *a* methyl ester (3)** isolated as brown-green band (10 mg, 2%), UV−vis λ_{max} (CH_2Cl_2) nm ($\varepsilon \times 10^4$) 412 (11.9), 509 (1.13), 539 (0.98), 619 (0.91), 678 (4.79); [lit.[47] λ_{max} (CH_2Cl_2) 412, 510, 540, 620, 678 (4.71)]. HRFABMS $C_{36}H_{38}N_4O_6$ $[MH]^+$ calcd 623.2869, obsd 623.2886.

The second major violet band was **bacteriopheophorbide *a* methyl ester (4)** (350 mg, 91%). UV−vis λ_{max} (CH_2Cl_2) nm ($\varepsilon \times 10^4$) 362 (10.5), 387 (5.19), 532 (2.76), 683 (1.12), 756 (6.27); [lit.[48] λ_{max} (CH_2Cl_2) 362, 387, 503, 530, 628, 680, 755]. HRFABMS $C_{36}H_{40}N_4O_6$ $[MH]^+$ calcd 625.3026, obsd 625.3043.

Bacteriopyropheophorbide *a* Methyl Ester (5). Bacteriopheophorbide *a* methyl ester, **4** (350 mg), was dissolved in collidine (20 mL) and refluxed under nitrogen for 2 h. The reaction mixture was diluted with hexane (500 mL), and the precipitate was filtered off and washed with hexane (100 mL). The residue was chromatographed on silica (eluent: dichloromethane−acetone, gradient 2−4% acetone) to separate a minor, faster-running brown band, identified as **3-acetyl-3-desvinyl-pyropheophorbide *a* methyl ester (6)** (10 mg, 3%), UV−vis λ_{max} (CH_2Cl_2) nm ($\varepsilon \times 10^4$) 412 (11.9), 509 (1.13), 539 (0.98), 619 (0.91), 678 (4.79); [lit.[48] λ_{max} ($CHCl_3$) 412, 510, 540, 620, 677]. HRFABMS $C_{34}H_{36}N_4O_4$ $[MH]^+$ calcd 565.2814, obsd 565.2803.

Bacteriopyropheophorbide *a* Methyl Ester (5). **5** was isolated as the major product. It was recrystallized from dichloromethane−hexane to give violet-black crystals (305 mg, 89%). UV−vis λ_{max} (CH_2Cl_2) nm ($\varepsilon \times 10^4$) 360 (10.2), 386 (5.23), 532 (2.69), 682 (1.09), 754 (6.17); [lit.[41] λ_{max} (CH_2Cl_2) 361, 387, 503, 530, 628, 681, 754]. FABMS *m*/*z* 567.3 ($[MH]^+$, 100%); HRFABMS $C_{34}H_{38}N_4O_4$ $[MH]^+$ calcd 567.2971, obsd 567.2956.

13²-Oxo-bacteriopyropheophorbide *a* Methyl Ester (8). Bacteriopyropheophorbide *a* methyl ester **5** (300 mg) was dissolved in THF (100 mL), and a suspension of lithium hydroxide (0.5 g) in water (4 mL) was added to the solution. The reaction mixture was vigorously stirred overnight at room temperature and then poured into water (0.5 L) containing acetic acid (5 mL). The product was extracted with a dichloromethane−THF mixture (1: 1). The combined extracts were washed with water, dried over sodium sulfate, and briefly treated with excess ethereal diazomethane; the solvent was evaporated in vacuum. The residue was separated on silica gel (eluent: dichloromethane−acetone, gradient 5−8% acetone), and product **8** was isolated as yellowish-brown band (215 mg, 68%). Dark-brown solid (from dichloromethane−hexane). UV−vis λ_{max} (CH_2Cl_2) nm ($\varepsilon \times 10^4$) 346 (7.12), 385 (8.73), 518 (1.89), 676 (0.89), 768 (8.97); ^{1}H NMR δ: 9.05 (s, 1H), 8.51 (s, 1H), 8.45 (s, 1H), 5.06 (dd, 1H), 4.56 (m, 2H), 4.02 (m, 1H), 3.65 (s, 3H), 3.52 (s, 3H), 3.44 (s, 3H), 3.18 (s, 3H), 2.58 (m, H), 2.48 (m, H), 2.24−2.12 (m, 4H), 1.84 (d, 3H), 1.78 (d, 3H), 1.13 (t, 3H), −0.29 and −1.03 (each br s, 2H); FABMS *m*/*z* 581.3 ($[MH]^+$, 100%); HRFABMS $C_{34}H_{36}N_4O_5$ $[MH]^+$ calcd 581.2739, obsd 581.2744. Anal. C: 70.24, H: 6.14, N: 9.68; req. C: 70.32, H: 6.25, N: 9.65.

Condensation of 13²-Oxo-bacteriopyropheophorbide *a* Methyl Ester (8) with 1,2-Phenylenediamine (9). 13²-Oxo-bacteriopyropheophorbide *a* methyl ester **8** (100 mg) was dissolved in pyridine (40 mL), and 1,2- phenylenediamine hydrochloride **9** (200 mg) was added. TFA (0.5 mL) was added, and the reaction mixture was heated at reflux for 1 h, monitoring the progress spectroscopically. The reaction mixture was diluted with water (500 mL) and extracted with dichloromethane. The organic layers were washed with water, dried over sodium sulfate, filtered, and evaporated in vacuum. The residue was chromatographed on silica (eluent: dichloromethane−acetone, gradient 2−5% acetone) to give two bands.

Quinoxalino-bacteriochlorin Methyl Ester (10). was isolated as a faster moving orange-red band. Yield: 33 mg (29%). Red-brown crystals (from dichloromethane−hexane), UV−vis λ_{max} (CH_2Cl_2) nm ($\varepsilon \times 10^4$) 357 (7.36), 387 (8.52), 582 (2.87), 759 (1.48), 816 (10.76); ^{1}H NMR δ: 9.24 (s, 2H), 8.51 (s, 2H), 7.96 (m, 2H), 7.49 (m, 2H), 5.03 (dd, 1H), 4.46 (q, 1H), 4.38 (m, 1H), 4.02 (m, 1H), 3.65 (s, 6H), 3.54 (s, 3H), 3.18 (s, 3H), 2.78 (m, H), 2.67 (m, H), 2.44−2.32 (m, 3H), 2.21 (m, 1H), 1.84 (m, 6H), 1.15 (t, 3H), 0.39 and −0.93 (each br s, 2H); ^{13}C NMR δ: 199.2, 174.0, 168.0, 167.0, 166.5, 164.2, 163.7, 154.8, 145.8, 141.3, 141.2, 141.1, 135.4, 134.2, 131.7, 131.0, 130.2, 129.4, 129.2, 128.2, 128.0, 125.0, 105.0, 100.3, 100.1, 97.3, 56.3, 52.4, 51.5, 48.4, 47.5, 33.3, 31.9, 31.4, 29.8, 23.9, 23.5, 13.5, 12.3, 10.8; FABMS *m*/*z* 653.3 ($[MH]^+$, 100%); HRFABMS $C_{40}H_{41}N_6O_3$ $[MH]^+$ calcd 653.33240, obsd 653.3258.

Benzimidazolo-bacteriochlorin (11). **11** was isolated as the second slower-eluting red-brown band. Yield: 59 mg (54%). Dark-purple needles (crystallized from dichloromethane−hexane), UV−vis λ_{max} (CH_2Cl_2) nm ($\varepsilon \times 10^4$) 374 (8.86), 423 (3.54), 553 (3.92), 773 (0.98), 850 (8.98); ^{1}H NMR δ: 9.26 (s, 2H), 8.71 (s, 1H), 8.59 (s, 1H), 8.06 (m, 1H), 7.86 (m, 1H), 7.30 (m, 2H), 5.43 (dd, 1H), 4.36 (m, 2H), 4.12 (m, 1H), 3.84 (s, 3H), 3.65 (s, 3H), 3.56 (s, 3H), 3.23 (s, 3H), 2.76 (m, 1H), 2.47 (m, 3H), 2.12 (m, 2H), 1.86 (m, 6H), 1.17 (t, 3H), −0.29 and −0.43 (each br s, 2H); ^{13}C NMR δ: 198.5, 173.9, 173.0, 168.9, 167.8, 165.6, 164.2, 148.1, 145.4, 136.9, 135.9, 135.3, 135.1, 132.5, 132.3, 131.3, 130.8, 125.1, 125.0, 119.8, 116.2, 115.9, 102.4, 102.3, 98.5, 97.8, 56.8, 54.9, 51.5, 48.1, 46.9, 33.1, 32.4, 31.1, 29.8, 24.1, 23.4, 13.6, 12.6, 10.8; FABMS *m*/*z* 639.3 ($[MH]^+$, 100%); HRFABMS $C_{40}H_{41}N_6O_4$ $[MH]^+$ calcd 669.3189, obsd 669.3173.

Perimidino-bacteriochlorin Methyl Ester (13). 13²-Oxo-bacteriopyropheophorbide *a* methyl ester **8** (50 mg) was dissolved in pyridine (20 mL), and 1,9-diaminonaphthalene hydrochloride (100 mg) was added. TFA (0.2 mL) was added, and the reaction mixture was heated at reflux for 1 h, monitoring the progress spectroscopically. The reaction mixture was diluted with water (300 mL) and extracted with dichloromethane. The combined organic layers were washed with water, dried, and evaporated in vacuum. The residue was chromatographed on silica (eluent: dichloromethane−acetone, gradient 2−5% acetone) to give the title product as dark-green crystals (from dichloromethane−hexane). Yield: 44 mg (79%). UV−vis λ_{max} (CH_2Cl_2) nm ($\varepsilon \times 10^4$) 357 (6.63), 398 (7.69), 534 (2.13), 660 (1.38), 740 (2.28), 829 (13.68); ^{1}H NMR δ: 9.28 (s, 2H), 8.76 (s, 1H), 8.63 (s, 1H), 8.17 (m, 1H), 7.34 (m, 5H), 5.46 (dd, 1H), 4.38 (m, 1H), 4.19 (m, 1H), 3.82 (s, 3H), 3.66 (s, 3H), 3.65 (s, 3H), 3.22 (s, 3H), 2.74 (m, 1H), 2.46 (m, 3H,), 2.10 (m, 2H), 1.83 (m, 6H), 1.18 (t, 3H), −0.69 and −0.83 (each br s, 2H); ^{13}C NMR δ: 198.6, 173.9, 171.7, 168.7, 166.8, 166.0, 165.6, 146.6, 139.9, 136.0, 135.4, 134.8, 134.4, 134.2, 133.7, 132.7, 132.1, 130.3, 127.7, 127.1, 123.7, 122.7, 121.5, 119.1, 118.3, 115.5, 101.2, 101.1, 99.8, 97.7, 57.0, 54.8, 51.5, 48.0, 47.0, 33.2, 32.2, 31.5, 29.9, 24.2, 23.5, 13.6, 13.3, 10.8; FABMS *m*/*z* 719.3 ($[MH]^+$, 100%); HRFABMS $C_{44}H_{43}N_6O_4$ $[MH]^+$ calcd 719.3346, obsd 719.3338.

Diazomethane Ring-Enlargement Reaction. 13²-Oxo-bacteriopyropheophorbide *a* methyl ester **8** (100 mg) was dissolved in dichloromethane (50 mL) and diazomethane, prepared from 2 g of *N*-methyl-*N*-nitroso-*p*-tolunesulfonamide (Diazald), was added. The reaction mixture was kept at room temperature in a sealed flask in the dark overnight, after which the solvent was evaporated in vacuum. Residue was chromatographed on silica (eluent: dichloromethane−acetone, gradient 3−5% acetone) to give the three products. The

fastest moving orange-red band was 13^2-methoxybacterioverdin methyl ester (**14**). Dark-red prisms (from dichloromethane–methanol). Yield: 30 mg (29%). UV–vis λ_{max} (CH_2Cl_2) nm ($\varepsilon \times 10^4$) 360 (9.56), 424 (5.52), 550 (2.52), 799 (2.08), 891 (5.18); ^{1}H NMR δ: 8.93 (s, 1H, 5-H), 8.16 (s, 1H, 20-H), 8.15 (s, 1H, 10-H), 6.89 (s, 1H, 13^1-H), 4.79 (dd, 1H, 17-H), 4.06 (s, 3H, 13^2-OCH_3), 3.98 (m, 1H, 7-H), 3.86 (q, 1H, 18-H), 3.77 (dd, 1H, 8-H), 3.62 (s, 3H, CO_2CH_3), 3.44 (s, 3H, 12-CH_3), 3.18 (s, 3H, 2-CH_3), 3.09 (s, 3H, $COCH_3$), 2.86 (m, H, 17^1_a-H), 2.56 (m, 1H, 8-CH_2, 17^2_b-H), 2.26 (m, 3H, 8-CH_2, $17^1_{a'}$-H,), 2.24 (m, 1H, $17^2_{b'}$-H), 1.73 (d, 3H, J = 8.0 Hz, 7-CH_3), 1.64 (d, 3H, J = 8.0 Hz, 18-CH_3), 1.06 (t, 3H, J = 7.6 Hz, 8^2-CH_3), 0.49 and 0.22 (each br s, 2H, 21, 23-NH); ^{13}C NMR δ: 198.3, 182.8, 174.5, 174.0, 168.7, 165.7, 162.8, 153.1, 141.4, 140.0, 133.6, 132.0, 130.7, 128.5, 127.6, 126.9, 104.0, 103.4, 101.8, 99.2, 57.6, 55.9, 55.7, 51.4, 46.1, 45.1, 32.9, 32.7, 30.1, 29.7, 28.9, 24.2, 23.4, 13.3, 10.8, 10.4; FABMS m/z 609.3 ([MH]$^+$, 100%); HRFABMS $C_{36}H_{40}N_4O_5$ [MH]$^+$ calcd 609.3077, obsd 609.3054.

The second band was identified **as 13^1-methoxybacterioverdin** (**15**) isolated as pink-red crystals. Yield: 45 mg (42%). UV–vis λ_{max} (CH_2Cl_2) nm ($\varepsilon \times 10^4$) 369 (10.43), 418 (5.12), 552 (3.72), 779 (2.46), 874 (7.85); ^{1}H NMR δ: 9.05 (s, 1H, 5-H), 8.46 (s, 1H, 10-H), 8.37 (s, 1H, 20-H), 5.95 (s, 1H, 13^2-H), 5.18 (dd, 1H, 17-H), 4.18 (s, 3H, 13^1-OCH_3), 4.16 (m, 1H, 7-H), 4.05 (q, 1H, 18-H), 3.90 (dd, 1H, 8-H), 3.65 (s, 3H, CO_2CH_3), 3.54 (s, 3H, 12-CH_3), 3.50 (s, 3H, 2-CH_3), 3.12 (s, 3H, $COCH_3$), 2.76 (m, H, 17^1_a-H), 2.52 (m, 1H, 8-CH_2, 17^2_b–H), 2.43 (m, 2H, 8-CH_2), 2.14 (m, 2H, $17^1_{a'}$-H, $17^2_{b'}$-H), 1.76 (d, 3H, J = 8.0 Hz, 7-CH_3), 1.64 (d, 3H, J = 8.0 Hz, 18-CH_3), 1.06 (t, 3H, J = 7.6 Hz, 8^2-CH_3), 0.36 (br s, 2H, 21,23-NH); ^{13}C NMR δ: 198.5, 189.8, 174.1, 173.6, 167.3, 166.3, 166.2, 165.1, 139.3, 137.1, 134.2, 133.9, 132.2, 129.9, 129.3, 122.1, 103.7, 103.6, 102.3, 101.4, 97.9, 57.2, 55.8, 54.8, 51.4, 47.2, 46.2, 33.0, 32.6, 30.8, 29.5, 24.2, 23.4, 13.5, 12.4, 10.8; FABMS m/z 609.3 ([MH]$^+$, 100%); HRFABMS $C_{36}H_{40}N_4O_5$ [MH]$^+$ calcd 609.3077, obsd 609.3066.

The third product was identified **13^3-methoxybacterioisoverdin** (**16**) isolated as blue-green crystals (from dichloromethane–methanol). Yield: 18 mg (16%). UV–vis λ_{max} (CH_2Cl_2) nm ($\varepsilon \times 10^4$) 371 (8.94), 395 (4.69), 596 (2.13), 766 (2.56), 865 (4.86); ^{1}H NMR δ: 8.95 (s, 1H, 5-H), 8.56 (s, 1H, 10-H), 8.36 (s, 1H, 20-H), 6.05 (s, 1H, 13^1-H), 4.78 (dd, 1H, 17-H), 4.22 (s, 3H, 13^3-OCH_3), 4.18 (m, 1H, 7-H), 4.06 (q, 1H, 18-H), 3.92 (dd, 1H, 8-H), 3.74 (s, 3H, 12-CH_3), 3.65 (s, 3H, CO_2CH_3), 3.51 (s, 3H, 2-CH_3), 3.16 (s, 3H, $COCH_3$), 2.56 (m, H, 17^1_a-H), 2.46 (m, 3H, 8-CH_2, 17^2_b-H), 2.24 (m, 2H, $17^1_{a'}$-H, $17^2_{b'}$-H), 1.79 (d, 3H, J = 8.0 Hz, 7-CH_3), 1.73 (d, 3H, J = 8.0 Hz, 18-CH_3), 1.09 (t, 3H, J = 7.6 Hz, 8^2-CH_3), 0.39 and 0.32 (each br s, 2H, 21, 23-NH); ^{13}C NMR δ: 198.4, 185.1, 173.6, 171.0, 169.9, 169.1, 168.9, 163.5, 136.7, 136.2, 134.0, 133.9, 133.8, 131.5, 122.0, 103.1, 102.6, 102.5, 101.4, 96.7, 56.4, 56.1, 54.6, 51.6, 48.5, 47.2, 33.1, 31.9, 31.8, 29.8, 29.6, 23.8, 23.0, 13.4, 12.2, 10.7; FABMS m/z 609.3 ([MH]$^+$, 100%); HRFABMS $C_{36}H_{40}N_4O_5$ [MH]$^+$ calcd 609.3077, obsd 609.3078.

Electrochemical Measurements. Cyclic voltammetry was carried out with an EG&G model 173 potentiostat/galvanostat. A homemade three-electrode cell was used that consisted of a platinum button or glassy carbon working electrode, a platinum wire counter-electrode, and a saturated calomel reference electrode (SCE). The SCE was separated from the bulk of the solution by a fritted-glass bridge of low porosity which contained the solvent/supporting electrolyte mixture. All potentials are referenced to the SCE. Low-temperature measurements were carried out by **immersing** the cell using a dry ice–acetone mixture bath.

Thin-layer UV–vis spectroelectrochemical experiments were performed using a home-built thin-layer cell, which has a transparent platinum networking electrode. Potentials were applied and monitored with an EG&G PAR model 173 potentiostat. High-purity N_2 from Trigas was used to deoxygenate the solution and was kept over the solution during each electrochemical and spectroelectrochemical experiment.

Tetra-*n*-butylammonium perchlorate (TBAP, ≥99%) was purchased from Fluka Chemical Co., recrystallized from ethyl alcohol, and dried under vacuum at 40 °C for at least one week prior to use. Dichloromethane (CH_2Cl_2, 99.8%) was purchased from EMD Chemicals Inc. and used as received.

Photophysical Measurements. Absorption spectra were recorded on a Hewlett-Packard 8453A diode array spectrophotometer. Time-resolved fluorescence and phosphorescence spectra were measured by a Photon Technology International GL-3300 with a Photon Technology International GL-302 nitrogen laser/pumped dye laser system equipped with a four-channel digital delay/pulse generator (Stanford Research System Inc. DG535) and a motor driver (Photon Technology International MD-5020). Excitation wavelengths were from 538 to 551 nm using coumarin 540A (Photon Technology International, Canada) as a dye. Fluorescence lifetimes were determined by a single exponential curve fit. Nanosecond transient absorption measurements were carried out using a Panther OPO-pumped Nd:YAG laser (Continuum, SLII-10, 4–6 ns fwhm) at 430 nm with the power of 3 mJ as an excitation source. Photoinduced events were estimated by using a continuous Xe lamp (150 W) and an InGaAs-PIN photodiode (Hamamatsu 2949) as a probe light and a detector, respectively. The output from the photodiodes and a photomultiplier tube was recorded with a digitizing oscilloscope (Tektronix, TDS3032, 300 MHz). The transient spectra were recorded using fresh solutions in each laser excitation. All experiments were performed at 298 K.

■ ASSOCIATED CONTENT

Ⓢ Supporting Information

^{1}H and ^{13}C NMR spectra of compounds, their transient absorption spectra and crystallographic details for compound **14** in CIF format and an ORTEP diagram of the conformer shown in Figure 4, tables of atom coordinates and absolute energies to document the theoretical calculations, transient absorption spectra and full author list of ref 43. This material is available free of charge via the Internet at http://pubs.acs.org.

■ AUTHOR INFORMATION

Corresponding Author

*ravindra.pandey@roswellpark.org (R.K.P.); kkadish@uh.edu (K.M.K.); fukuzumi@chem.eng.osaka-u.ac.jp (S.F.); akozyrev@nanosyn.com (A.K.)

Notes

The authors declare no competing financial interest.

■ ACKNOWLEDGMENTS

Support from the NIH (CA127369, CA55791, R.K.P.), Robert A. Welch Foundation (Grant E-680, K.M.K.) and a Global COE program from the Ministry of Education, Culture, Sports, Science and Technology, Japan (to S.F.), and KOSEF/MEST through WCU projects (R31-2008-000-10010-0), Korea is gratefully acknowledged. We are thankful to Dr. Fajer, Brookhaven National Lab (BNL) for X-ray analysis of one of the bacteriochlorin analogues. The help rendered by Dr. Mark Renner (ZINDO calculations) and Michael Becker for crystallizing compound **14** is also appreciated. X-ray data and were measured at beamline X25 of the National Synchrotron Light Source and supported by the Center for Research Resources of the NIH, and the Office of Biological and Environmental Research and Basic Energy Sciences of the U.S. Department of Energy, a Grant-in-Aid (No. 20108010 to S.F. and 23750014 to K.O.). We thank Dr. Avinash Phadke (Achillion Pharmaceuticals, Inc.) for valuable discussions, the late Dr. James L. Alderfer, RPCI, Buffalo, for 2D/ROSEY measurements and Dr. James G. Pavlovich (UCSB) for help in obtaining mass-spectra and Drs. A. A.Tsygankov and N. Zorin (ISP, Puschino-on-Oka, Russian Federation) for a supply of *Rh. sphaeroides* biomass. A part of the experimental chemistry/

analysis was performed at the former Miravant Medical Technology, Inc. Santa Barbara, CA 93117.

REFERENCES

(1) Ethirajan, M.; Chen, Y.; Penny, J.; Pandey, R. K. *Chem. Soc. Rev.* **2011**, *40*, 340−362.
(2) Dolmans, E. J. G. J.; Kadambi, A.; Hill, J. S.; Waters, C. A.; Robinson, B. C.; Walker, J. P.; Fukumura, D.; Jain, R. K. *Cancer Res.* **2002**, *62*, 2151.
(3) Pandey, R. K.; Herman, C. *Chem. Ind. (London)* **1998**, 739.
(4) Bonnett, R. *Chem. Soc. Rev.* **1995**, 19 and references therein.
(5) Wilson, B. C. *CIBA Found. Symp.* **1989**, *52*, 741.
(6) Jasat, A.; Dolphin, D. *Chem. Rev.* **1997**, *97*, 2267 and references therein.
(7) Lash, T. D.; Werner, T. M.; Thompson, M. L.; Manley, J. D. *J. Org. Chem.* **2001**, *66*, 3152.
(8) Sessler, J. L.; Hemmi, G.; Mody, T. D.; Murai, T.; Burrell, A.; Young, S. W. *Acc. Chem. Res.* **1994**, *27*, 43 and references therein.
(9) Vogel, E.; Koch, P.; Hou, X.-L.; Lex, J.; Lausman, M.; Kisters, M.; Aukauloo, M.; Richard, P.; Guilard, R. *Angew. Chem., Int. Ed. Engl.* **1993**, *32*, 1600.
(10) Kozyrev, A. N.; Efimov, A. V.; Efremova, O. A.; Perepyolkin, P. Yu.; Mironov, A. F. *Proc. SPIE-Int. Soc. Opt. Eng.* **1994**, *2325*, 297.
(11) Phadke, A. S.; Robinson, B. C.; Barkigia, K. M.; Fajer, J. *Tetrahedron* **2000**, 7661.
(12) (a) Hynninen, P. H. In *The Chlorophylls*; Scheer, H., Ed.; CRC Press: Roca Baton, FL, 1991; pp 146−209. (b) Chen, Y.; Li, G.; Pandey, R. K. *Curr. Org. Chem.* **2004**, *8*, 1105. (c) Yang, E.; Kirmaier, C.; Krayer, M.; Taniquchi, M.; Kim, H. J.; Diers, J. R.; Bocian, D. F.; Lindsey, J. S.; Hollen, D. *J. Phys. Chem. B* **2011**, *115*, 10801. (d) Kim, H. J.; Lindsey, J. S. *J. Org. Chem.* **2005**, *70*, 5475. (e) Tamiaki, H.; Miyatake, T.; Tanikaga, R.; Holzwarth, A.; Schaffner, K. *Angew. Chem., Int. Ed. Engl.* **1996**, *35*, 772 and references therein. (f) Sasaki, S.; Tamiaki, H. *J. Org. Chem.* **2006**, *71*, 2648.
(13) Yon-Hin, P.; Wijesekera, T. P.; Dolphin, D. *Tetrahedron Lett.* **1991**, *32*, 2875.
(14) (a) Pandey, R. K.; Shiau, F.-Y.; Ramachandaran, K.; Dougherty, T. D.; Smith, K. M. *J. Chem. Soc., Perkin Trans. 1* **1992**, 1377. (b) Ethirajan, M.; Joshi, P.; William, W. H., Jr.; Ohkubo, K.; Fukuzumi, S.; Pandey, R. K. *Org. Lett.* **2011**, *13*, 1956−1959.
(15) Robinson, B. C.; Barkigia, K. M.; Renner, M. W.; Fajer, J. *J. Phys. Chem. B.* **1999**, *103*, 7324.
(16) Kay, C. W.; Conti, F.; Fuhs, M.; Plato, M.; Weber, S.; Bordignon, E.; Carbonera, D.; Robinson, B. C.; Renner, M. W.; Fajer, J. *J. Phys. Chem. B* **2002**, *106*, 2769.
(17) Robinson, B. C. *Tetrahedron* **2000**, *56*, 6005.
(18) Morgan, A. R.; Skalkos, D.; Garbo, G. D.; Keck, R. W.; Selman, S. H. *J. Med. Chem.* **1991**, *34*, 2126.
(19) (a) Pandey, R. K.; Goswami, L. N.; Chen, Y.; Grushuk, A.; Missert, J. R.; Oseroff, A.; Dougherty, T. J. *Lasers Surg. Med.* **2006**, *38*, 445 and references therein. (b) Pandey, R. K.; Zheng, G. In *The Porphyrin Handbook*; Kadish, K. M., Smith, K. M., Guilard, R., Eds.; Academic Press, San Diego, 2000; Vol. *6*, pp 157−230.
(20) Beems, E. M.; Dubbelman, T. M. A. R.; Lugtenberg, J.; Van Best, J. A.; Smeets, M. F. M. A.; Boegheim, J. P. *Photochem. Photobiol.* **1987**, *45*, 639.
(21) Henderson, B. W.; Sumlin, A. B.; Owczarczak, B. L.; Dougherty, T. J. *J. Photochem. Photobiol. B* **1991**, *10*, 303.
(22) Kozyrev, A. N.; Zheng, G.; Dougherty, T. J.; Smith, K. M.; Pandey, R. K. *Tetrahedron Lett.* **1996**, *37*, 6431.
(23) (a) Kozyrev, A. N.; Dougherty, T. J.; Pandey, R. K. *Chem. Commun.* **1998**, 481. (b) Joshi, P.; Ethirajan, M.; Goswami, L. N.; Srivatsan, A.; Missert, J. R.; Pandey, R. K. *J. Org. Chem.* **2011**, *76*, 8629.
(24) Mironov, A. F.; Kozyrev, A. N.; Brandis, A. S. *Proc. SPIE-Int. Soc. Opt. Eng.* **1992**, 202.
(25) Wasielewski, M. R.; Svec, W. A. *J. Org. Chem.* **1980**, *45*, 1969.
(26) Fischer, H.; Lambrecht, R.; Mittenzwei, H. *Z. Physiol. Chem.* **1938**, *253*, 1.
(27) (a) Pandey, R. K., Kozyrev, A. N.; Zheng, L. U.S. Patent 7,147,840, 2006. (b) Fukuzumi, S.; Ohkubo, K.; Zheng, X.; Chen, Y.; Pandey, R. K.; Zhan, R.; Kadish, K. M. *J. Phys. Chem. B* **2008**, *112*, 2738.
(28) Kozyrev, A. N.; Alderfer, J. L.; Srikrishnan, T.; Pandey, R. K. *J. Chem. Soc., Perkin Trans. 1* **1998**, 837.
(29) Kozyrev, A. N.; Suresh, V.; Das, S.; Senge, M. O.; Shibata, T.; Alderfer, J. L.; Dougherty, T. J.; Pandey, R. K. *Tetrahedron* **2000**, *56*, 3353.
(30) Pandey, R. K.; Shiau, F.-Y.; Ramachandaran, K.; Dougherty, T. D.; Smith, K. M. *J. Chem. Soc., Perkin Trans. 1* **1992**, 1377.
(31) Morgan, A. R.; Rampersaud, A.; Keck, R. W.; Selman, S. *Photochem. Photobiol.* **1987**, *46*, 441.
(32) Kozyrev, A. N.; Alderfer, J. L.; Dougherty, T. J.; Pandey, R. K. *Chem. Commun.* **1998**, 1083.
(33) Kozyrev, A. N.; Alderfer, J. L.; Dougherty, T. J.; Pandey, R. K. *Angew. Chem., Int. Ed.* **1999**, *38*, 126.
(34) ZINDO-S method. In *HyperChem*, release 7; HyperCube, Inc.: Gainesville, FL, 2002.
(35) Fukuzumi, S.; Ohkubo, K.; Chen, Y.; Pandey, R. K.; Zhan, R.; Shao, J.; Kadish, K. M. *J. Phys. Chem. A* **2002**, *106*, 5105.
(36) Geskes, C.; Hartwich, G.; Scheer, H.; Maentele, W.; Heinze, J. *J. Am. Chem. Soc.* **1995**, *117*, 7776.
(37) Kadish, K. M.; Caemelbecke, V.; E.; Royal, G. In *The Porphyrin Handbook*; Kadish, K. M., Smith, K. M., Guilard, R., Eds.; Academic Press: San Diego, CA, 2000; Vol. *8*; pp 1−97.
(38) (a) Fukuzumi, S.; Suenobu, T.; Patz, M.; Hirasaka, T.; Itoh, S.; Fujitsuka, M.; Ito, O. *J. Am. Chem. Soc.* **1998**, *120*, 8060. (b) Fukuzumi, S.; Ohkubo, K.; Imahori, H.; Guldi, D. M. *Chem.—Eur. J.* **2003**, *9*, 1585. (c) Kawashima, Y.; Ohkubo, K.; Fukuzumi, S. *J. Phys. Chem. A* **2012**, *116*, 8942.
(39) Noy, D.; Fiedor, L.; Hartwich, G.; Scheer, H.; Scherz, A. *J. Am. Chem. Soc.* **1998**, *120*, 3684.
(40) Frank, B.; Nonn, A. *Angew. Chem., Int. Ed. Engl.* **1995**, *34*, 1795.
(41) Seidal, D.; Lynch, V.; Sessler, J. L. *Angew. Chem., Int. Ed.* **2002**, *41*, 1422.
(42) Becke, A. D. *J. Chem. Phys.* **1993**, *98*, 5648.
(43) Frisch, M. J.; et al. *Gaussian 09*, Revision A.02; Gaussian, Inc.: Wallingford CT, 2009(see Supporting Information for the complete reference).
(44) Dennington II, R.; Keith, T.; Millam, J.; Eppinnett, K.; Hovell, W. L.; Gilliland, R. *Gaussview*, ver. 3.09; Semichem, Inc.: Shawnee Mission, KS, 2003.
(45) Ethirajan, M.; Joshi, P.; William, W. H.; Ohkubo, K.; Fukuzumi, S.; Pandey, R. K. *Org. Lett.* **2011**, *13*, 1956.
(46) Crossley, M. J.; Langford, S. J.; Parashar, J. K.; Burn, P. L. *J. Chem. Soc., Chem. Commun.* **1998**, 1921.
(47) Hartwich, G. A.; Fiedor, L.; Simonin, I.; Cmiel, E.; Schafer, W.; Noy, D.; Scherz, A.; Scheer, H. *J. Am. Chem. Soc.* **1998**, *120*, 3675.
(48) Kozyrev, A. N.; Perepyolkin, P. Y.; Mironov, A. F. *Proc. SPIE-Int. Soc. Opt. Eng.* **1993**, 186.